Principle and Analysis of a Novel Linear Synchronous Motor with Half-Wave Rectified Self Excitation

Jun OYAMA, Tsuyoshi HIGUCHI, Takashi ABE, Shotaro KUBOTA and Tadashi HIRAYAMA
Department of Electrical and Electronic Engineering, Nagasaki University
1-14 Bunkyo-machi, Nagasaki, 852-8521 Japan
Phone: +81-95-847-1111(Ext. 2665), Fax: +81-95-846-7379
E-mail:oyama@net.nagasaki-u.ac.ip

Abstract

Principle and analysis of a new type LSM are presented. The motor is based on half-wave rectified brushless excitation. The field winding is short-circuited through a diode and the armature winding is conventional 3-phase windings. As the field flux is controllable by varying armature current, field weakening operation is possible in high speed region. The experimental machine is designed and built. The characteristics are estimated theoretically and the inductance is compared with measured value.

Key words: Linear Synchronous Motor, Half Wave Rectified Self Excitation.

1 Introduction

Linear synchronous motors (LSM) have been widely used in various industry applications, such as, transportation system, NC machine tools and home appliances. A permanent magnet (PM) type LSM is used in general application, because the field excitation is provided without DC power supply and the efficiency is high. If a d-axis current big enough to offset against the PM flux is provided, the field weakening operation becomes possible in high speed region. However, a loss by the d-axis current causes a drop in motor efficiency especially at low torque.

In the previous papers, we proposed a half-wave rectified brushless synchronous motor [1] [2] [3]. Balanced 3-phase currents in the 3-phase armature windings of conventional synchronous motor produce the mmf that has constant amplitude and rotates at synchronous angular velocity w. If the amplitude of the balanced 3-phase currents is modulated by an alternating wave with bias frequency w_b, the produced mmf pulsates at w_b and rotates at w. This pulsating mmf induces the emf with bias frequency w_b in the field winding. The field excitation of the half-wave rectified brushless synchronous motor is obtained by rectifying the emf with a diode connected in series with the field winding.

In the previous paper [4], we proposed a new type LSM, which is based on the half-wave rectified brushless excitation principle. In this paper, we describe the self-excitation and thrust generation principle of the novel linear synchronous motor with half-wave rectified self excitation. We also show the experimental machine and then estimate the performance by simulation.

2 Principle of New LSM

2.1 Motor Construction

Fig. 1 shows a model of the proposed new LSM with half-wave rectified self excitation. The LSM consists of followings;

(1) A LSM mover whose field winding is short circuited through a diode.
(2) A LSM stator with three phase armature windings.
(3) A PWM inverter

2.2 Voltage Equation

Fig. 2 shows a dq-axis model of the new LSM. The field winding is short-circuited through a diode. The dq-axis voltage equation is

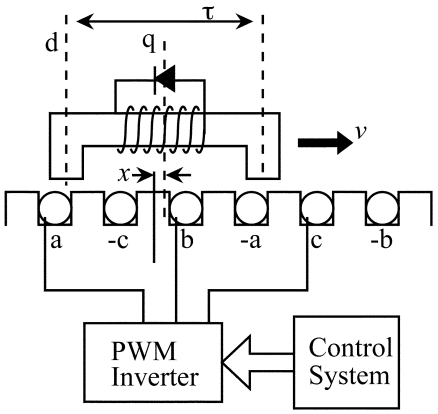

Fig. 1. Configuration of New LSM.

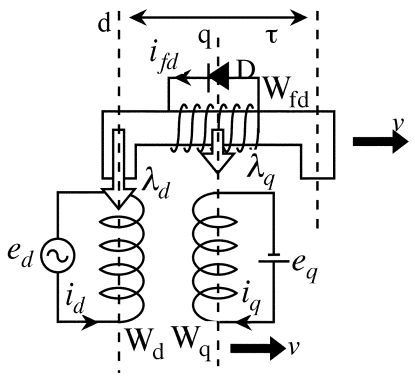

Fig. 2. Equivalent Model on the dq-Axis.

$$\left.\begin{aligned} e_d &= (d/dt)l_d - w\,l_q + r_a i_d \\ e_q &= (d/dt)l_q + w\,l_d + r_a i_q \\ e_{fd} &= (d/dt)l_{fd} + r_a i_{fd} \end{aligned}\right\} \cdots\cdots (1)$$

The flux linkages are expressed in terms of self-inductance L and mutual-inductance M as follows,

$$\left.\begin{aligned} l_d &= L_d i_d + M_{fd} i_{fd} \\ l_q &= L_q i_q \\ l_{fd} &= M_{fd} i_d + L_{fd} i_{fd} \end{aligned}\right\} \cdots\cdots (2)$$

Where, e_d is the d-axis voltage, e_q is the q-axis voltage, e_{fd} is the field voltage. i_d is the d-axis current, i_q is the q-axis current, i_{fd} is the field current. r_a is the stator winding resistance, r_{fd} is the field winding resistance. l_d is the d-axis flux linkage with the stator winding, l_q is the q-axis flux linkage, l_{fd} is the flux linkage with the field winding.

The w is synchronous angular velocity. The mover position x in Fig. 1 is the position between the stator a-axis and the mover q-axis. The synchronous angular velocity w and synchronous mover velocity v_s are as follow;

$$wt = \frac{p}{t} v_s t = \frac{p}{t} x \cdots\cdots (3)$$

The origin, $x = 0$, is defined where the stator a-axis is inline with the mover q-axis.

2.3 Principle of Self Excitation and Thrust Generation

Fig. 3 illustrates the principle of the half-wave rectified self-excitation and thrust generation. The following 3-phase currents, which synchronized with mover position, are supplied to the 3-phase stator windings of Fig. 1;

$$\left.\begin{aligned} i_a &= A_f(t)\sin wt + \sqrt{2} I_t \cos wt \\ i_b &= A_f(t)\sin(wt - 2p/3) + \sqrt{2} I_t \cos(wt - 2p/3) \\ i_c &= A_f(t)\sin(wt - 4p/3) + \sqrt{2} I_t \cos(wt - 4p/3) \end{aligned}\right\} \cdots\cdots (4)$$

The first term on the right-hand side of equations (4) is excitation current, which varies with sine of the mover position x and whose amplitude is a modulation function $A_f(t)$. $A_f(t)$ is a triangular wave function with the effective value of I_f and bias frequency w_b. The second term of the equation is thrust current component.

The d-axis current becomes;

$$i_d = \sqrt{(3/2)}\, A_f(t) \cdots\cdots (5)$$

We can, therefore, obtain such a travelling field as if produced by a single-phase current i_d in the d-axis winding W_d which moves synchronously with the mover. As a result, a flux linkage $M_{fd} i_d$ is generated on the mover d-axis.

The field current i_{fd} is induced in the field winding to keep the maximum value of the flux. The flux linkage l_{fd} is the sum of flux linkages; $M_{fd} i_d$ provided by the stator excitation current and $L_{fd} i_{fd}$ by the mover field current. If inductance of the circuit is large enough, l_{fd} is kept constant and held to it's maximum by the diode.

The q-axis current becomes;

$$i_q = \sqrt{3} I_t \cdots\cdots (6)$$

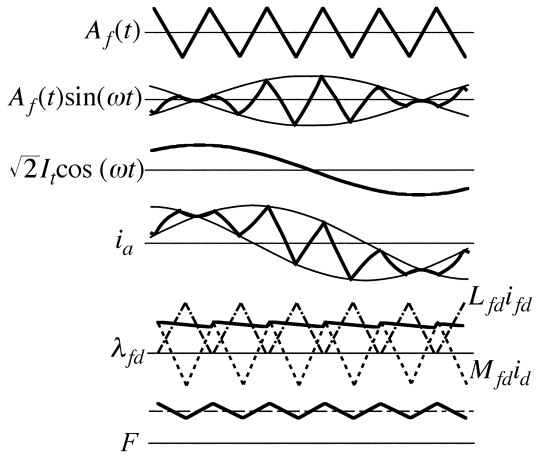

Fig. 3. Principle of Thrust Generation.

We can obtain such a travelling field as if produced by a direct current i_q to the q-axis winding W_q which moves synchronously with the mover. Then the thrust is obtained from the following equation.

$$F = \frac{p}{t}(l_d i_q - l_q i_d) \quad \cdots\cdots (7)$$

Assuming that r_a and r_{fd} equal zero, then the thrust is

$$F = \frac{p}{t}\left(3\sqrt{\frac{3}{2}}(1-s)L_d I_f I_t + \frac{3}{\sqrt{2}}(s L_d - L_q)A_f(t) I_t\right) \quad \cdots\cdots (8)$$

Though a pulsating component exists in this thrust as shown in Fig. 3, it is not serious problem for practical usage by suitable choosing the bias frequency w_b and $(s L_d - L_q)$.

3 Experimental machine

Fig. 4 illustrates the designed experimental motor. Table 1 shows the specifics and constants of the experimental machine.

Fig. 5 shows photos of the new type LSM and the mover, which we built. The full length of a stator is 2m. The cushion is attached on both side in order to protect the mover. A wire type linear encoder is attached to the mover.

4 Analysis

4.1 Procedure

Design or analysis is carried out by the following sequence.

Table 1. Design Parameters of Experimental Motor.

Rated Output	0.8 kW
Rated Voltage	200 V
Rated Current	4 A
Rated Speed	0.5 m/s
Number of Poles	4
Stator Length	1990 mm
Pole Pitch	60 mm
Stack Height	50 mm
Windings	Double Layer Distributed Pitch
Winding Diameter	0.8mm
Stator Winding	85 turns / pole
Mover Winding	300 turns

(I) The circuit parameters such as self- and mutual- inductances of stator armature windings and a mover field winding are estimated using the FEM analysis. Magnetic saturation of the core is taken into account.

(II) The equivalent circuit is created using the circuit parameters obtained at step (I) and then the performances are computed by a circuit simulator.

4.2 Inductance and flux linkage

By FEM analysis, we obtain the maximum value L_{max} and minimum value L_{min} of self inductances of the stator armature windings, the maximum value M_{max} and minimum value M_{min} of mutual inductances between the armature windings, the maximum mutual inductance M_f between the armature and the mover field windings, and the maximum self inductance L_{fd} of the field winding. Fig. 6 shows the FEM model of the experimental motor. The number of elements is 10753 and the number of nodes is 10509. Table 2 shows the estimated inductances. As FEM software, we use "ANSYS", Cybernet Co..

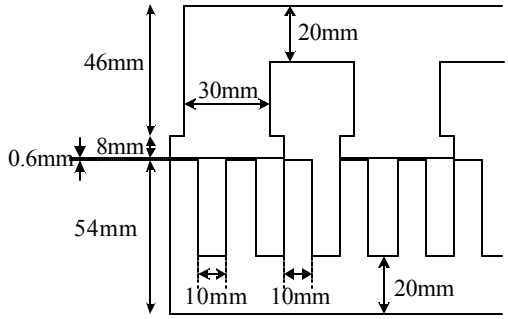

Fig. 4. Dimensions of Experimental Motor.

(a) The appearance of LSM.

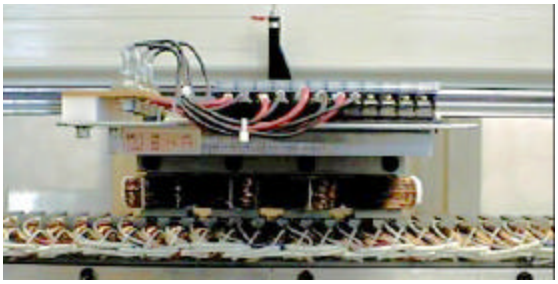

(b) The mover

Fig. 5. Photo of Experimental Motor.

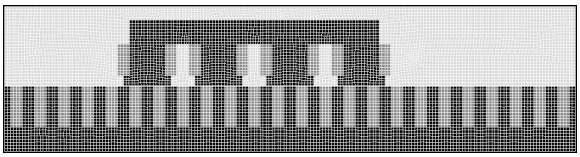

Fig. 6. FEM Model of Experimental Motor.

Table 2. Inductance of Experimental Motor.

L_{max}	125.5mH	L_{min}	97.1mH
M_{max}	69.4mH	M_{min}	40.4mH
M_f	240.5mH	L_{fd}	976.7mH
R_s	12.48Ω	R_m	2.38Ω

Here, assuming that each flux linkages vary with sinusoidal waveform, the flux linkages are expressed as follows,

$$\left.\begin{aligned} [l_{abc}] &= [L_{ss}][i_{abc}] + [M_{sf}]i_{fd} \\ l_{fd} &= [M_{sf}]^t [i_{abc}] + L_{fd} i_{fd} \end{aligned}\right\} \cdots\cdots\cdots\cdots (9)$$

Where,

$$[L_{ss}] = \begin{bmatrix} L_{aa} & M_{ab} & M_{ac} \\ M_{ab} & L_{bb} & M_{bc} \\ M_{ac} & M_{bc} & L_{cc} \end{bmatrix}$$

$$= \begin{bmatrix} L_a - L_m \cos 2wt & -M_s - L_m \cos 2\left(wt - \frac{1}{3}p\right) & -M_s - L_m \cos 2\left(wt - \frac{2}{3}p\right) \\ -M_s - L_m \cos 2\left(wt - \frac{1}{3}p\right) & L_a - L_m \cos 2\left(wt - \frac{2}{3}p\right) & -M_s - L_m \cos 2wt \\ -M_s - L_m \cos 2\left(wt - \frac{2}{3}p\right) & -M_s - L_m \cos 2wt & L_a - L_m \cos 2\left(wt - \frac{1}{3}p\right) \end{bmatrix}$$

$$[M_{sf}] = \begin{bmatrix} M_{af} \\ M_{bf} \\ M_{cf} \end{bmatrix} = \begin{bmatrix} M_f \sin wt \\ M_f \sin\left(wt - \frac{2}{3}p\right) \\ M_f \sin\left(wt - \frac{4}{3}p\right) \end{bmatrix}$$

$$\left.\begin{aligned} L_a &= (L_{\max} + L_{\min})/2 \\ L_m &= (L_{\max} - L_{\min})/2 \\ M_s &= (M_{\max} + M_{\min})/2 = (L_a - l_s)/2 \end{aligned}\right\} \cdots\cdots\cdots\cdots (10)$$

L_{max} : Stator Self-Inductance ($x = t / 2$)
L_{min} : Stator Self-Inductance ($x = 0$)
M_{max} : Stator Mutual-Inductance ($x = t / 3$)
M_{min} : Stator Mutual-Inductance ($x = 5t / 6$)
l_s : Stator Leakage Inductance
M_f : Maximum Stator-Mover Mutual Inductance
L_{fd} : Maximum Mover Self-Inductance

On the experiment, at first, DC resistances of the stator and mover windings are measured by the voltage drop method. Next, the inductances are measured using AC current (60Hz, 1.0A). Fig. 7 shows the measured inductances. The black square mark shows the theoretical inductance using FEM. The experimental results agree well with the theoretical one. Some errors between them may depend on subtle difference of boundary conditions and iron core parameter or effect of the punch hole which is used to fix the iron core.

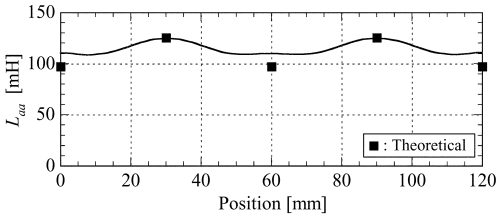

(a) Stator winding self-inductance.

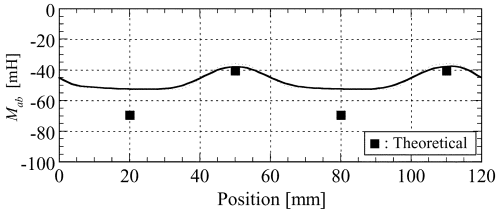

(b) Stator winding mutual-inductance.

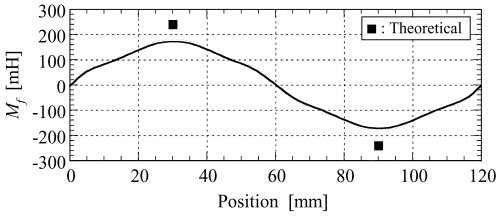

(c) Stator and mover mutual-inductance.

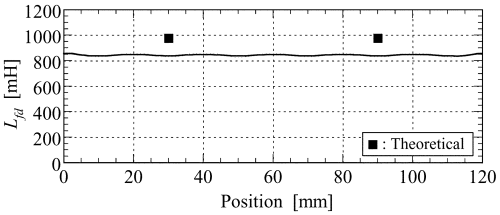

(d) Mover winding self-inductance.

Fig. 7. Measured and Estimated Inductances.

4.3 Performance characteristics

For computing the performance characteristics, the circuit simulator "SIMPLORER", Ansoft Co., is used. The model of not only the LSM but also the control system is created, and the time varying characteristics of current, flux linkage, and thrust are computed.

Using the flux linkage of the equation (9), the 3-phase voltage are written as follows.

$$\left.\begin{aligned}[e_{abc}] &= [R_s][i_{abc}] + p[l_{abc}] \\ e_{fd} &= r_{fd} i_{fd} + p\, l_{fd}\end{aligned}\right\} \quad \cdots\cdots\cdots\cdots\cdots\cdots (11)$$

Where, p is differential operator. Since each inductance is a function of mover position, the equation (11) changes as follows.

$$\begin{aligned}[e_{abc}] &= [R_s][i_{abc}] + p\left([L_{ss}][i_{abc}] + [M_{sf}]i_{fd}\right) \\ &= [R_s][i_{abc}] + \left(p[L_{ss}]\right)[i_{abc}] + [L_{ss}]\left(p[i_{abc}]\right) \\ &\quad + \left(p[M_{sf}]\right)i_{fd} + [M_{sf}]\left(p i_{fd}\right)\end{aligned} \quad \cdots\cdots\cdots\cdots\cdots\cdots (12)$$

$$\begin{aligned}e_{fd} &= r_{fd} i_{fd} + p\left([M_{sf}]^t[i_{abc}] + L_{fd} i_{fd}\right) \\ &= r_{fd} i_{fd} + \left(p[M_{sf}]^t\right)[i_{abc}] + [M_{sf}]^t\left(p[i_{abc}]\right) \\ &\quad + L_{fd}\left(p i_{fd}\right)\end{aligned} \quad \cdots\cdots\cdots\cdots\cdots\cdots (13)$$

On the basis of the above equation, the LSM model was constituted using the circuit simulator and is shown in Fig. 8. In this model, the 3-phase armature windings and the field winding short-circuited by a diode are modeled by analog elements. The Bemf_a, Bemf_b, and so on modeled by voltage source are back emf developed on the each winding. The back emf and thrust are defined by the equations in the simulator. But these equations are omitted here.

Fig. 9 shows the control system model. The control system consists of a gate drive circuit and a PWM inverter.

The thrust characteristics are computed using above simulation model. In this simulation, the excitation amplitude command I_f = 1.0A, the thrust current command I_t = 4.0A, synchronous mover velocity v_s = 0.5m/s (f = 4.17Hz), bias frequency w_b = 60Hz. Fig. 10 shows the simulated waveforms of command current and inverter output current. Inverter output current is well followed to command value at inverter input voltage V_{in} = 180V. Fig. 11 shows the field winding current, field winding flux linkage and thrust waveform. Though a pulsating component exists in this thrust, average thrust is 55.7N at thrust current command I_t = 4.0A.

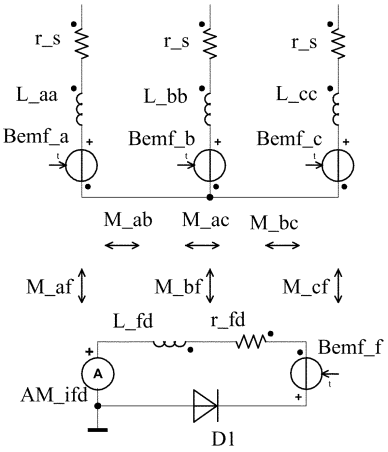

Fig. 8. Simulation Model of Experimental Motor.

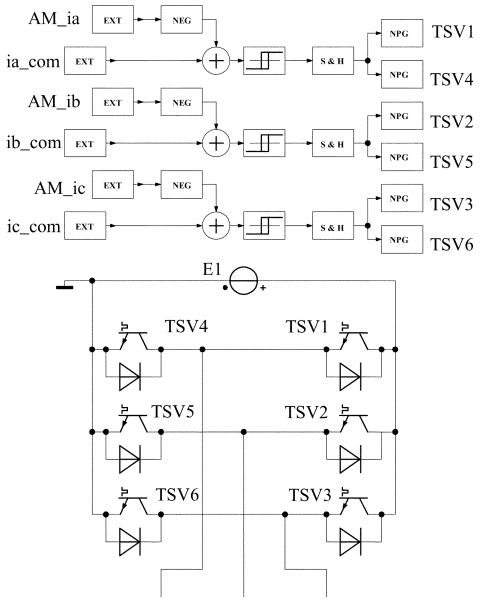

Fig. 9. Simulation Model of Control System.

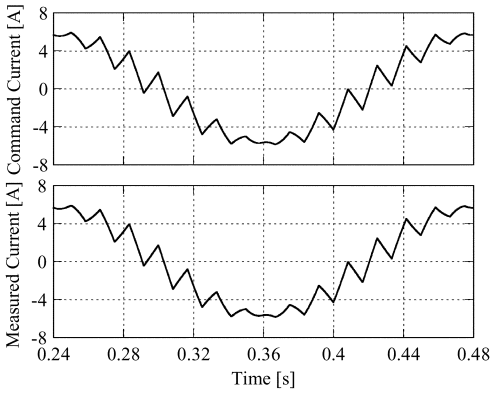

Fig. 10. Stator Current of a-Phase.

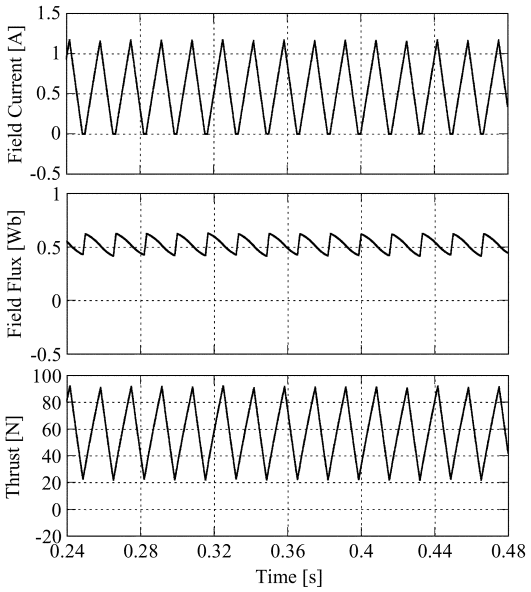

Fig. 11. Simulation Results.

Fig. 12 shows the performances including effect of varying the excitation amplitude command from I_f = 1.2A to 0.8A at t = 0.48s. Speed reference v_s = 0.5m/s (Frequency f = 4.2 Hz) and thrust current command I_t = 4.0 A. The field current i_{fd} induced in the field winding pulsates at bias frequency w_b= 60Hz. It is confirmed that the field current, flux linkage and thrust can be controlled easily by the excitation command.

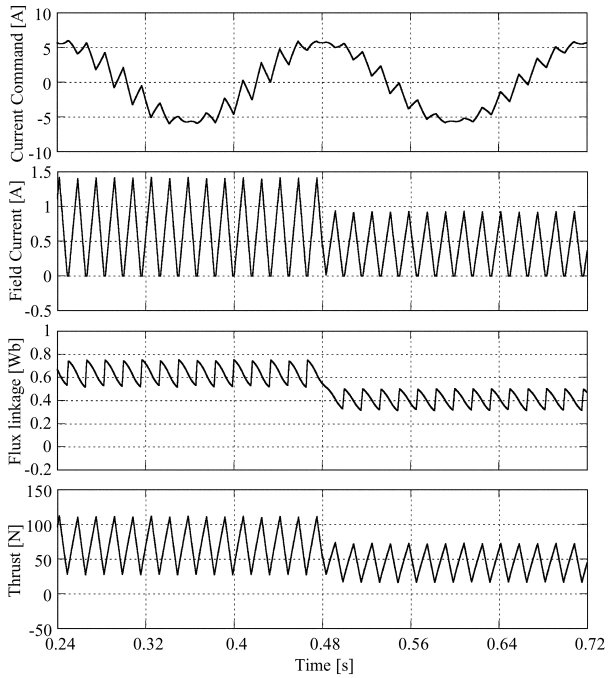

Fig. 12. Field Flux Control.

5 Conclusions

A novel linear synchronous motor with half-wave rectified self-excitation was proposed and the principle, analysis and experimental LSM were described. The inductance was computed using the FEM and compared with the experimental results. The performance characteristics were simulated by the circuit simulator. Now, the drive system of this LSM is under test. We will report the output characteristic s test results and the optimum design for reducing the pulsating thrust in future.

Reference

[1] J. Oyama, S. Toba, T. Higuchi and E. Yamada, "*The Characteristics of Half-Wave Rectified Brushless Synchronous Motor*", Proc. of Beijing ICEM, Vol. 2, pp.654-657, 1987.

[2] J. Oyama, T. Higuchi, T. Abe and E. Yamada, "*Characteristics of Half-Wave Rectified Brushless Synchronous Motor with Permanent Magnets*", Proc. of European Conference on Power Electronics and Applications, vol.3, pp.1513-1517, 1989.

[3] J. Oyama, T. Higuchi, T. Abe and E. Yamada, "*Analysis of Half-Wave Rectified Brushless Synchronous Motor with Permanent Magnets*", Conference Record of IEEE Industry Applications Society Annual Meeting, pp.781-786, 1990.

[4] J. Oyama, T. Higuchi, T. Abe, H. Tanaka and E. Yamada, "*A Novel Linear Synchronous Motor with Half-Wave Rectified Self Excitation*", The Third International Symposium on Linear Drives for Industry Applications, pp.144-148, 2001.10